Lagrangian reconstructions of temperature and velocity in a model of surface ocean turbulence

Stefano Berti [1] and Guillaume Lapeyre [2]

[1] Laboratoire de Mécanique de Lille, Université de Lille 1

[2] Laboratoire de Météorologie Dynamique, ENS Paris

Inversion of SWOT ocean observations
16/6/2014 - Toulouse, France

Motivation

- SSH spectra seem to be quite flat (k^{-4}) $\Rightarrow$ submesoscales should be very energetic

- Vorticity dominated by structures below 10 km (vorticity $\sim \partial_x^2$ SSH)

- At these scales: noise may be large $\Rightarrow$ SWOT signal may not be dynamically interesting (e.g. to compute vertical velocities)

- However SWOT will provide better velocities than currently available at scales above 30 km

Motivation

- Different datasets of upper ocean properties are available: SSH, SST, Chlorophyll, ...

- The combined use of different products can allow to access submesoscales (1 km) starting from data at 20 km or more

Motivation

- Different datasets of upper ocean properties are available: SSH, SST, Chlorophyll, ...

- The combined use of different products can allow to access submesoscales (1 km) starting from data at 20 km or more

A possible method to reconstruct temperature and velocity

- SST reconstruction by Lagrangian advection
- Surface Quasi Geostrophy $\Rightarrow$ 3D velocities at submesoscales

▶ **Here: test in idealized numerical simulations**

Motivation

• Different datasets of upper ocean properties are available: SSH, SST, Chlorophyll, ...

• The combined use of different products can allow to access submesoscales (1 km) starting from data at 20 km or more

A possible method to reconstruct temperature and velocity

• SST reconstruction by Lagrangian advection
• Surface Quasi Geostrophy $\Rightarrow$ 3D velocities at submesoscales

▶ **Here: test in idealized numerical simulations**

• Using mesoscale velocities derived from SWOT signal could considerably improve the reconstruction of submesoscale features

Lagrangian reconstruction method

$C(\boldsymbol{x}, t)$: tracer field; $\boldsymbol{u}(\boldsymbol{x}, t)$: velocity field

conservation along Lagrangian the flow

$$\begin{cases} \partial_t C + \boldsymbol{u} \cdot \boldsymbol{\nabla} C = 0 \\ \dfrac{d\boldsymbol{x}}{dt} = \boldsymbol{u}(\boldsymbol{x}(t), t) \end{cases}$$

used in atmospheric sciences since the 1990's [e.g., Sutton et al. 1994]

Lagrangian reconstruction method

$C(\boldsymbol{x}, t)$: tracer field; $\boldsymbol{u}(\boldsymbol{x}, t)$: velocity field

conservation along Lagrangian the flow

$$\begin{cases} \partial_t C + \boldsymbol{u} \cdot \nabla C = 0 \\ \dfrac{d\boldsymbol{x}}{dt} = \boldsymbol{u}(\boldsymbol{x}(t), t) \end{cases}$$

advection of particles: $\dfrac{d\boldsymbol{x}_p}{dt} = \boldsymbol{u}(\boldsymbol{x}_p(t), t); \quad p = 1, ..., N_p$

old position: $\boldsymbol{x}_p(t - \tau_a)$

new position: $\boldsymbol{x}_p(t)$

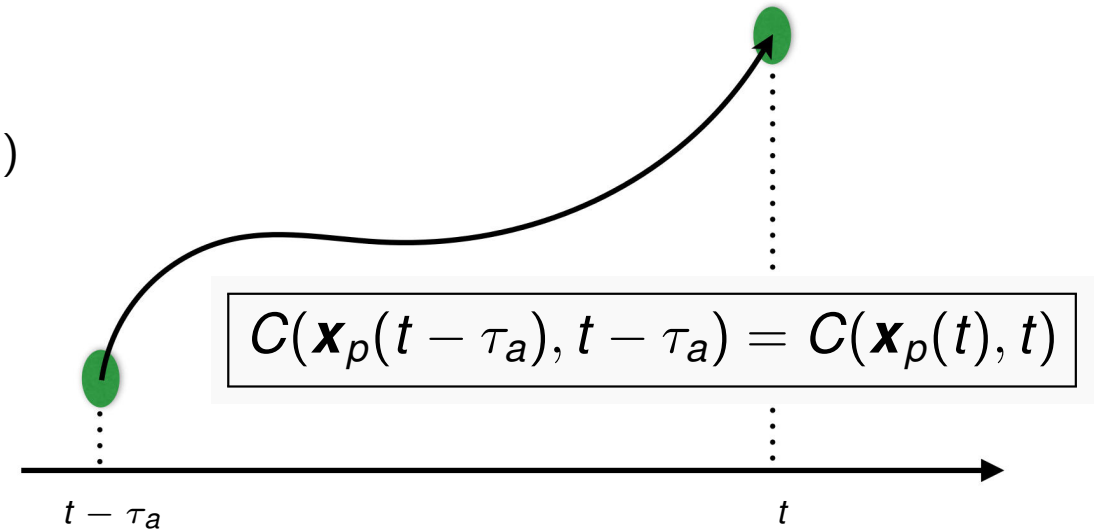

used in atmospheric sciences since the 1990's [e.g., Sutton et al. 1994]

Lagrangian reconstruction method

$C(\boldsymbol{x}, t)$: tracer field; $\boldsymbol{u}(\boldsymbol{x}, t)$: velocity field

conservation along Lagrangian the flow $\begin{cases} \partial_t C + \boldsymbol{u} \cdot \nabla C = 0 \\ \dfrac{d\boldsymbol{x}}{dt} = \boldsymbol{u}(\boldsymbol{x}(t), t) \end{cases}$

advection of particles: $\dfrac{d\boldsymbol{x}_p}{dt} = \boldsymbol{u}(\boldsymbol{x}_p(t), t); \quad p = 1, ..., N_p$

old position: $\boldsymbol{x}_p(t - \tau_a)$

new position: $\boldsymbol{x}_p(t)$

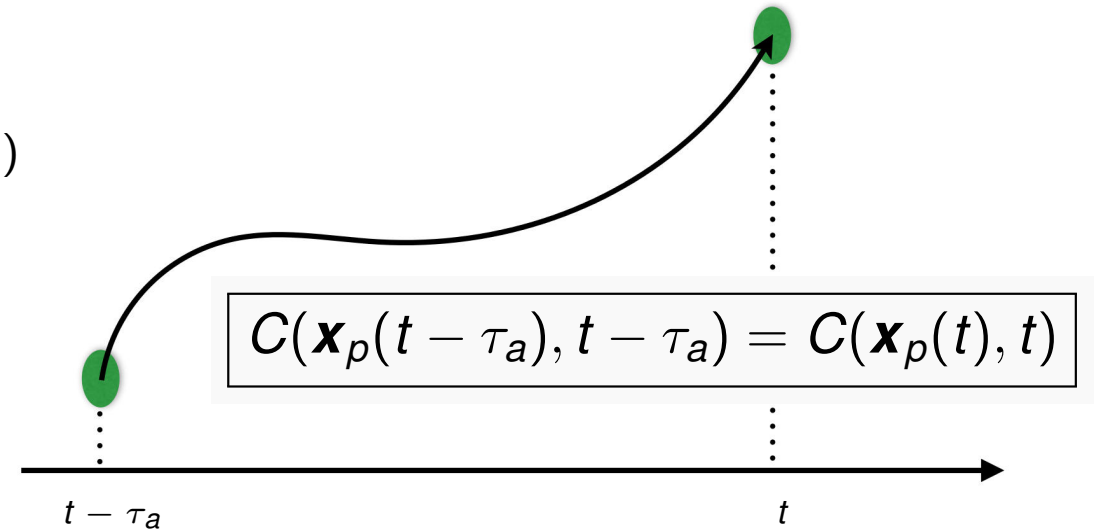

low-resolution tracer field $\rightarrow$ chaotic advection $\rightarrow$

$\rightarrow$ higher resolution tracer field at new particle positions (reconstruction)

used in atmospheric sciences since the 1990's [e.g., Sutton et al. 1994]

Lagrangian reconstruction method

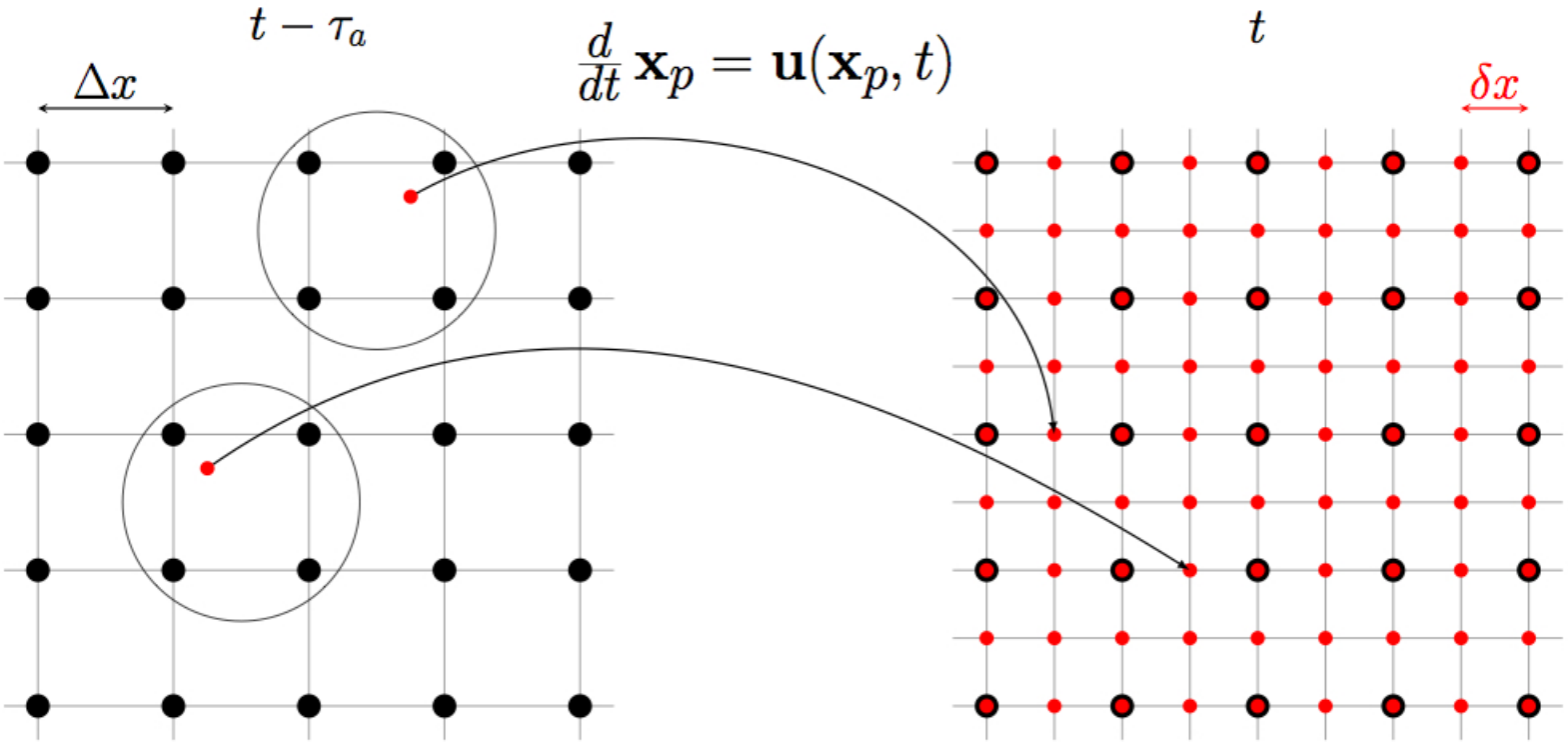

- For each particle at $\boldsymbol{x}_p$ ($p = 1, ..., N_p$) at time t:
  - reverse trajectory to time $t - \tau_a$
  - spatial interpolation on the low-resolution grid to obtain C at time $t - \tau_a$
  - the value of C at time $t - \tau_a$ is assigned to the particle

Numerical simulations of SQG turbulence

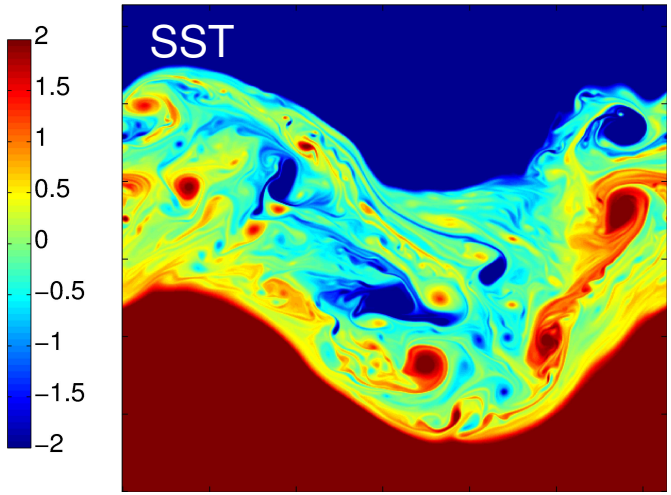

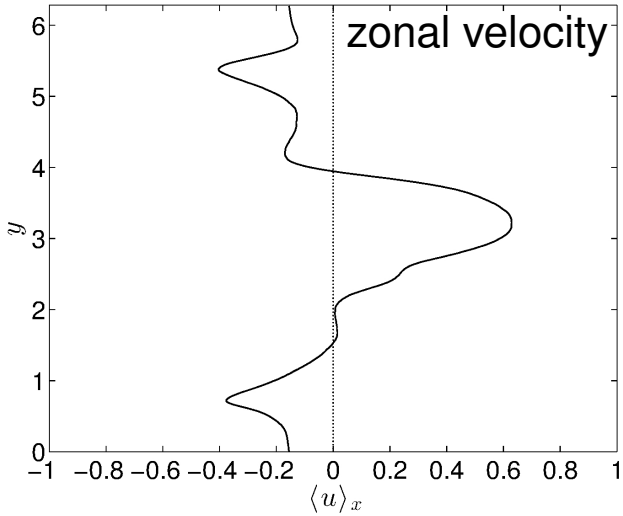

[Berti and Lapeyre 2014]

$$\partial_t \Theta + \boldsymbol{u} \cdot \boldsymbol{\nabla} \Theta = F + D$$

with $\boldsymbol{u} = (u, v) = (u, v) = (-\partial_y \psi, \partial_x \psi)$

SST: $\Theta = \theta + \beta y$

Large scale gradient: $\beta = \frac{\partial \Theta}{\partial y}$

Forcing: $F = -\kappa \left(\langle \theta \rangle_x - \bar{\theta} \right)$ relaxation to a given temperature profile $\bar{\Theta}(y)$

Dissipation: $D = -f_d(y)\theta(\boldsymbol{x}, t)/\tau$ with $f_d(y) = 1$ only close to the boundaries in y

SQG: $\hat{\psi} = \hat{\theta}/k$ at the surface [Held et al. 1995]

correctly represents meso and submesoscale dynamics of upper ocean layers

[LaCasce and Mahadevan 2006; Lapeyre and Klein 2006; Isern-Fontanet et al. 2006,2008; Klein et al. 2008]

Numerical procedure

Tracer to reconstruct $\rightarrow$ $C \equiv \Theta$ (SST)

- SQG simulations

  high-resolution fields $\boldsymbol{u}_{hr}(\boldsymbol{x}, t), \Theta_{hr}(\boldsymbol{x}, t)$ $\quad \delta x = \frac{2\pi}{N_{hr}} \approx 0.012$; $N_{hr} = 512$

  observations: degradation of $\Theta_{hr}(\boldsymbol{x}, t) \rightarrow \Theta_{lr}(\boldsymbol{x}, t)$

  by filtering wavenumbers $k > k_d = 20$; $\quad \Delta x = \frac{16\pi}{N_{hr}} \approx 0.1$

  $\Theta_{lr}(\boldsymbol{x}, t) \rightarrow \boldsymbol{u}_{lr}(\boldsymbol{x}, t)$ $\quad$ low-resolution velocity

- Reconstructions

  Lagrangian advection of Θ_{lr} by $\boldsymbol{u}_{lr}$ $\quad$ N_p particles; typically $\sqrt{N_p} = N_{hr}$

  obtain reconstructed SST: $\Theta_{rec}(\boldsymbol{x}, t)$

  using SQG: $\Theta_{rec}(\boldsymbol{x}, t) \rightarrow \boldsymbol{u}_{rec}(\boldsymbol{x}, t)$

Reconstruction of SST fields

(1) **original** ($\delta x = 2\pi / N_{hr}$); $t_0 = 50$

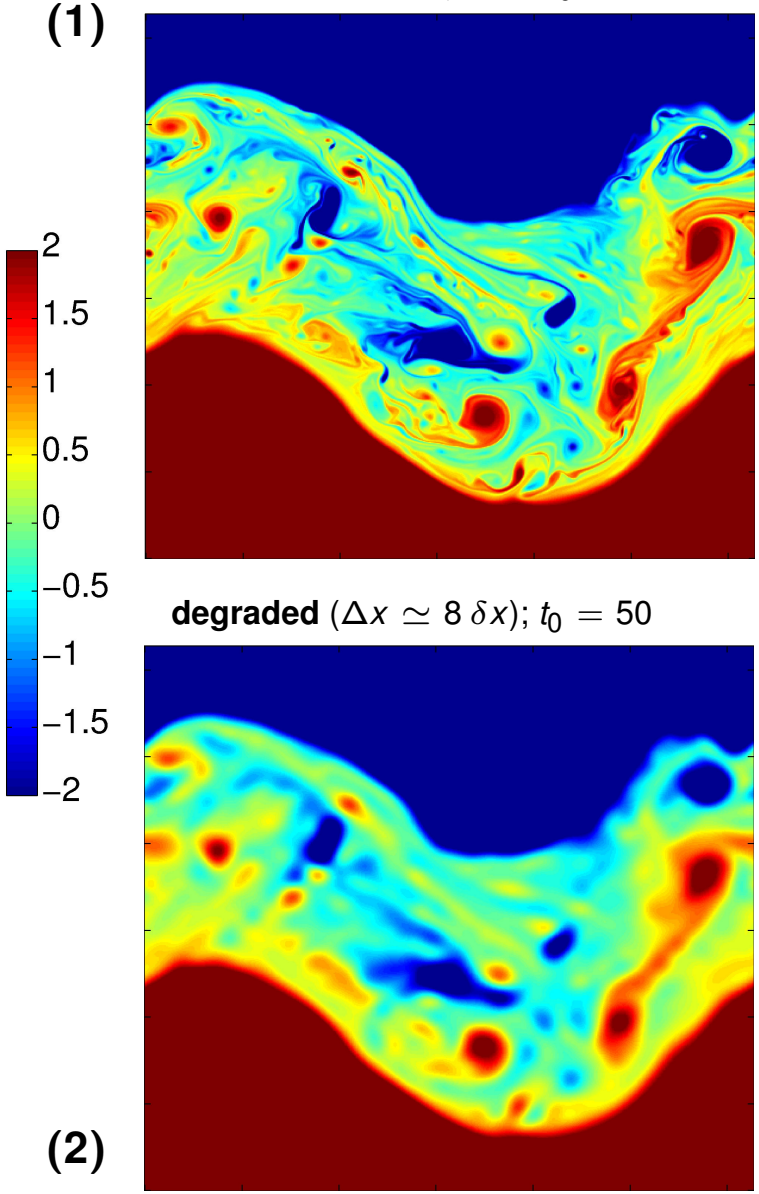

degraded ($\Delta x \simeq 8\,\delta x$); $t_0 = 50$

(2)

(1) Direct numerical simulations (SQG) with $N_{hr} = 512$

(2) Degradation of both $\boldsymbol{u}$ and Θ at $N_{lr} \simeq N_{hr}/8$

(3) Lagrangian reconstruction with $N_p = N_{hr}^2$ particles

Reconstruction of SST fields

(1)

original ($\delta x = 2\pi / N_{hr}$); $t_0 = 50$

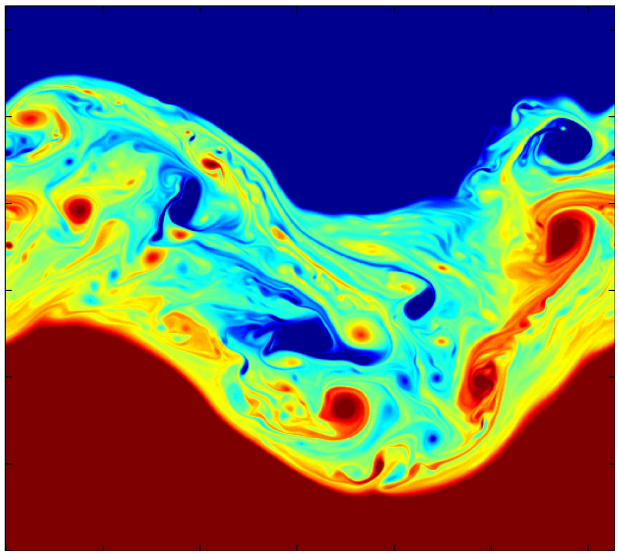

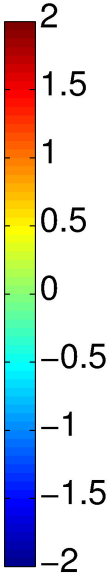

degraded ($\Delta x \simeq 8\,\delta x$); $t_0 = 50$

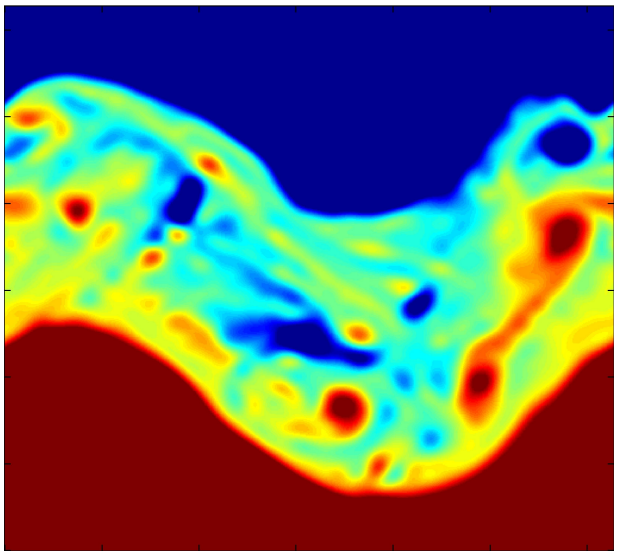

(2)

reconstructed ($\sqrt{N_p} = N_{hr}$); $t_0 = 50$

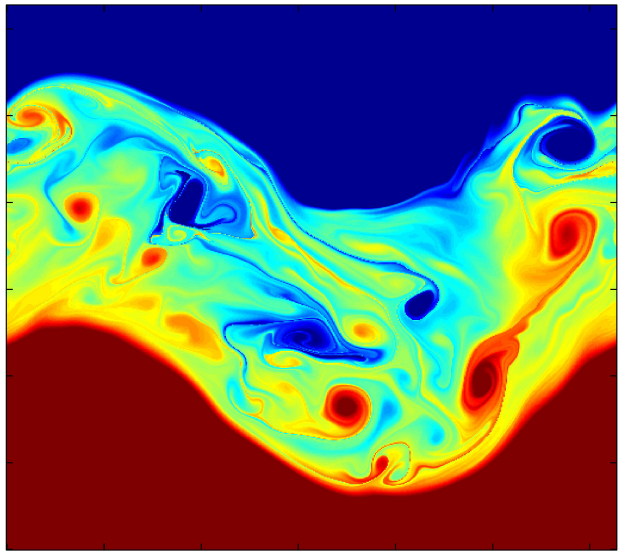

(3)

backward advection with $\tau_a = 7.5\,\tau_{lr}$

best for:
$5\,\tau_{lr} < \tau_a < 10\,\tau_{lr}$

$\tau_{lr} = \langle \zeta_{lr}^2 \rangle^{-1/2} \approx 0.2$ eddy turnover time of low-resolution velocity

(1) Direct numerical simulations (SQG) with $N_{hr} = 512$

(2) Degradation of both $\boldsymbol{u}$ and Θ at $N_{lr} \simeq N_{hr}/8$

(3) Lagrangian reconstruction with $N_p = N_{hr}^2$ particles

Gradients of SST fields

original ($\delta x = 2\pi / N_{hr}$); $t_0 = 50$

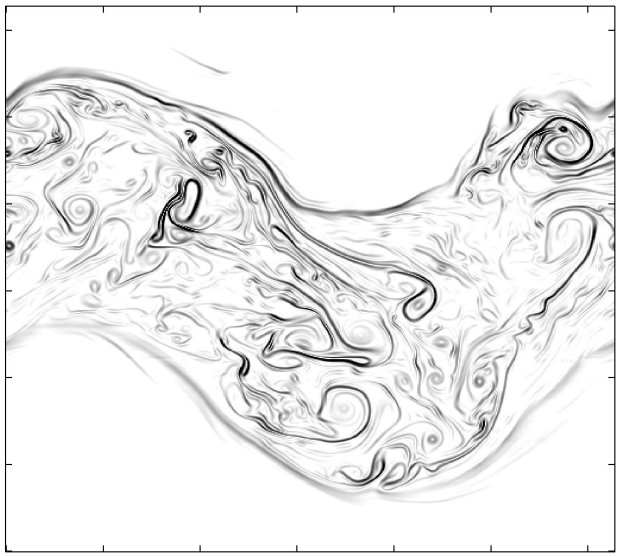

degraded ($\Delta x \simeq 8\,\delta x$); $t_0 = 50$

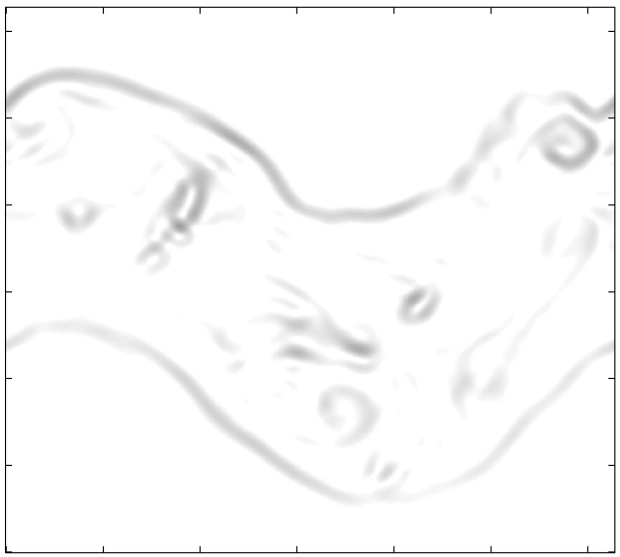

intensity of tracer gradients $|\boldsymbol{\nabla}\theta'| = \sqrt{(\partial_x\theta')^2 + (\partial_y\theta')^2}$

- detection of fronts
- maps of Finite Time Lyapunov Exponents

  [Crisanti et al. 1991, Lapeyre 2002]

Gradients of SST fields

original ($\delta x = 2\pi / N_{hr}$); $t_0 = 50$

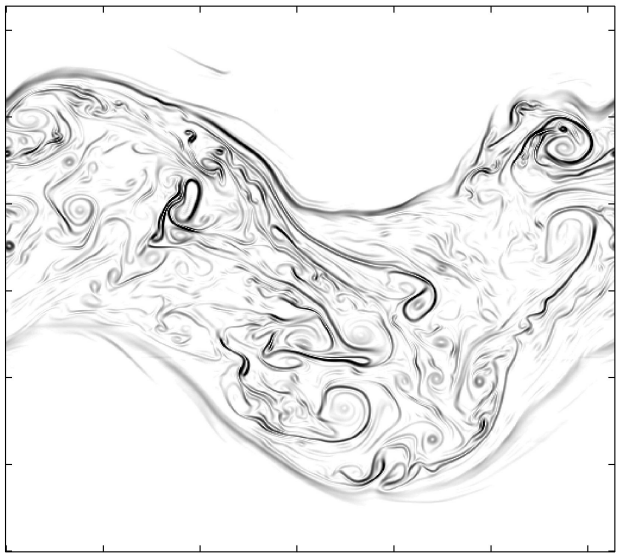

reconstructed ($\sqrt{N_p} = N_{hr}$); $t_0 = 50$

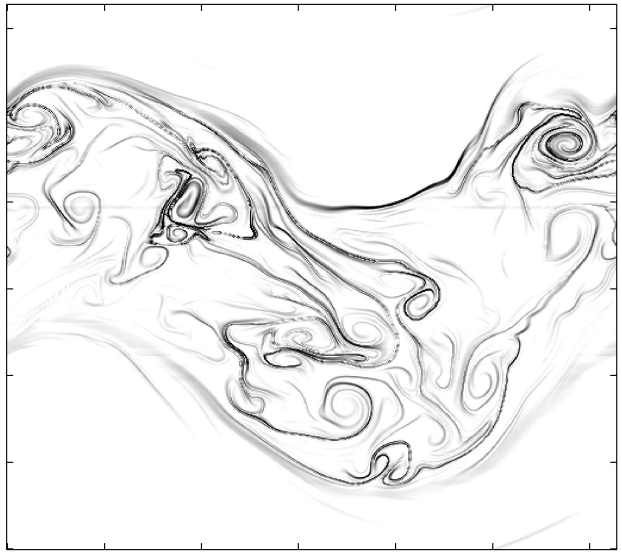

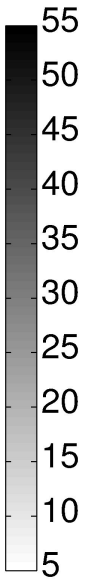

degraded ($\Delta x \simeq 8\,\delta x$); $t_0 = 50$

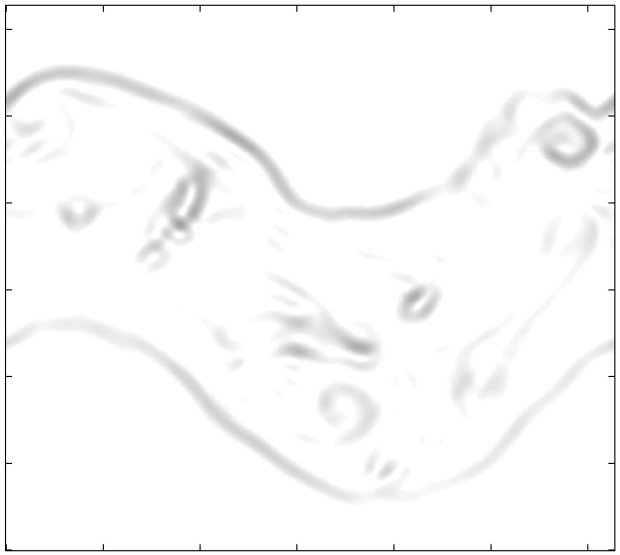

backward advection

with $\tau_a = 8\,\tau_{lr}$

best for:

$5\,\tau_{lr} < \tau_a < 10\,\tau_{lr}$

intensity of tracer gradients $|\nabla\theta'| = \sqrt{(\partial_x\theta')^2 + (\partial_y\theta')^2}$

- detection of fronts
- maps of Finite Time Lyapunov Exponents

  [Crisanti et al. 1991, Lapeyre 2002]

Probability distribution of SST gradients

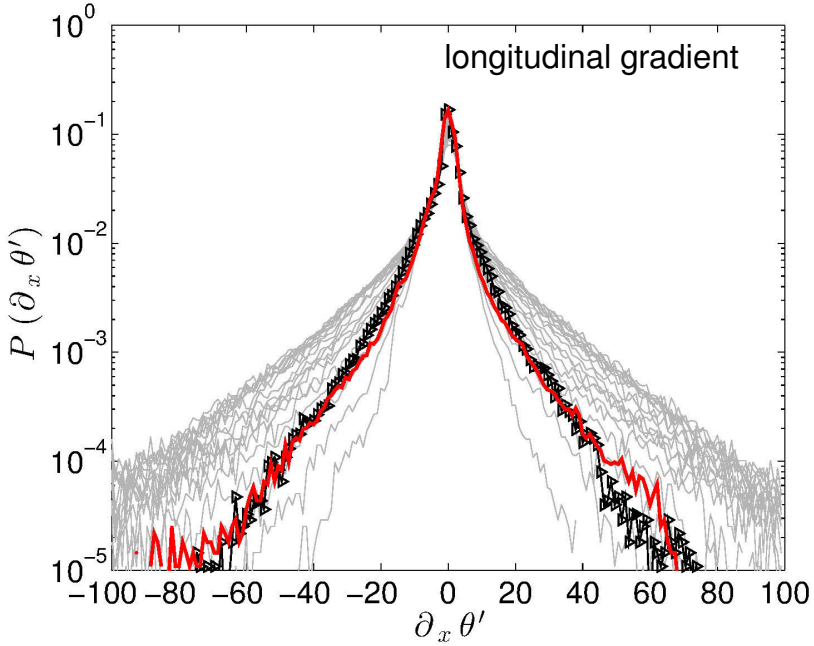

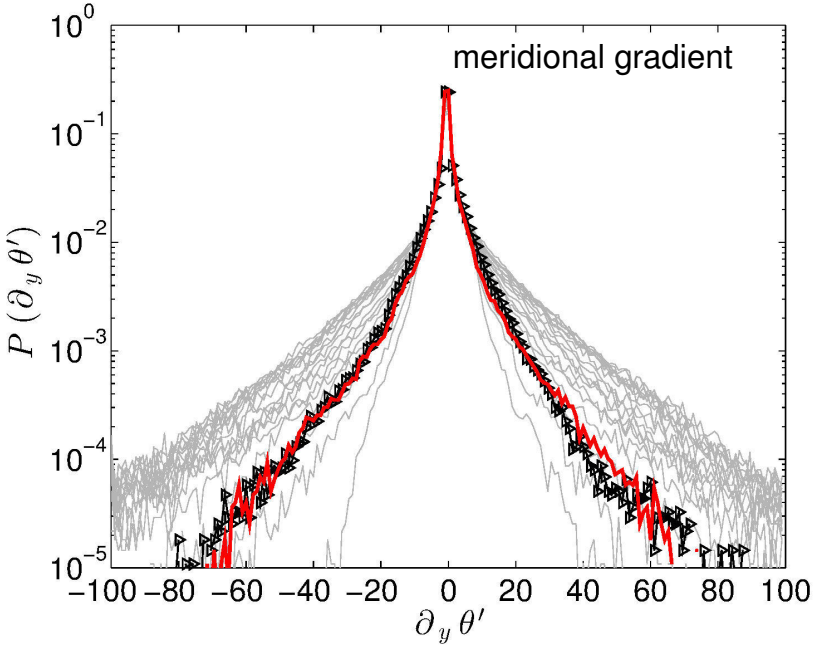

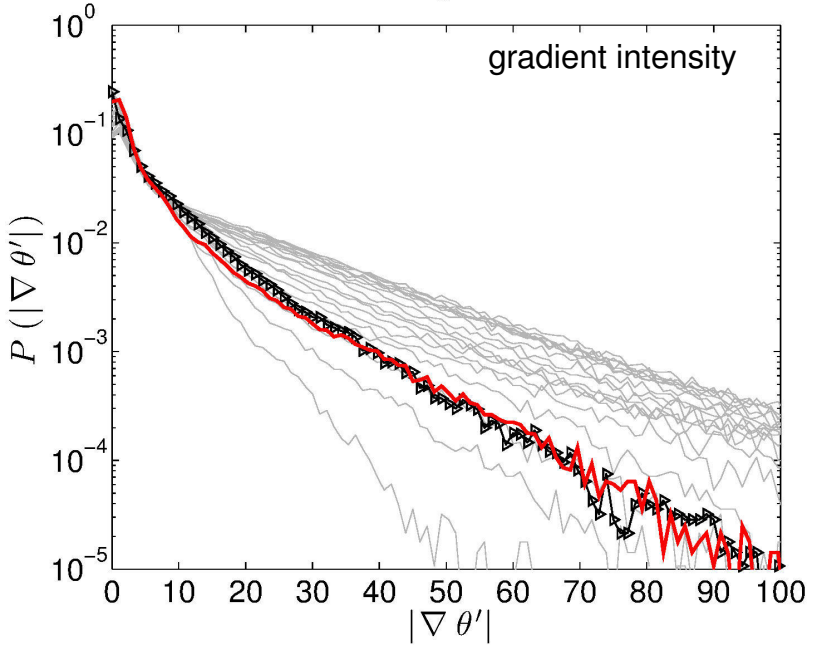

- original at t_0
- reconstructed with $\tau_a = (2.5, 5, 7.5, ..., 50)\,\tau_{lr}$
- reconstructed with $\tau_a = 8\,\tau_{lr}$

Reconstruction of the flow field

$$\partial_t \Theta + \boldsymbol{u} \cdot \boldsymbol{\nabla} \Theta = F + D \qquad \text{with } \boldsymbol{u} = (u, v) = (u, v) = (-\partial_y \psi, \partial_x \psi)$$

SST: $\Theta = \theta + \beta y$

- from θ using the SQG relation $\Rightarrow$ $\psi(x, y, t)$ and $\boldsymbol{u}(\boldsymbol{x}, t)$
- + "omega" equation relating w with $\boldsymbol{u}$ and θ:

$$\boldsymbol{\nabla}^2 w + \frac{\partial^2 w}{\partial z^2} = \boldsymbol{\nabla} \cdot [(\boldsymbol{\nabla} \boldsymbol{u}) \boldsymbol{\nabla} \theta]$$

$$\Longrightarrow \quad \left.\begin{array}{l} \text{vertical velocity } w \\ \\ \text{divergence } D \end{array}\right\} \text{ are also available}$$

Reconstruction of the flow field

SQG $\Rightarrow$ surface streamfunction: $\hat{\psi} = \hat{\theta}/k$

reconstruction of small-scale SST: $\theta(x, y) \longrightarrow$ flow field: $\psi(x, y)$

original; $t_0 = 50$ **degraded**; $t_0 = 50$ **reconstructed**; $t_0 = 50$

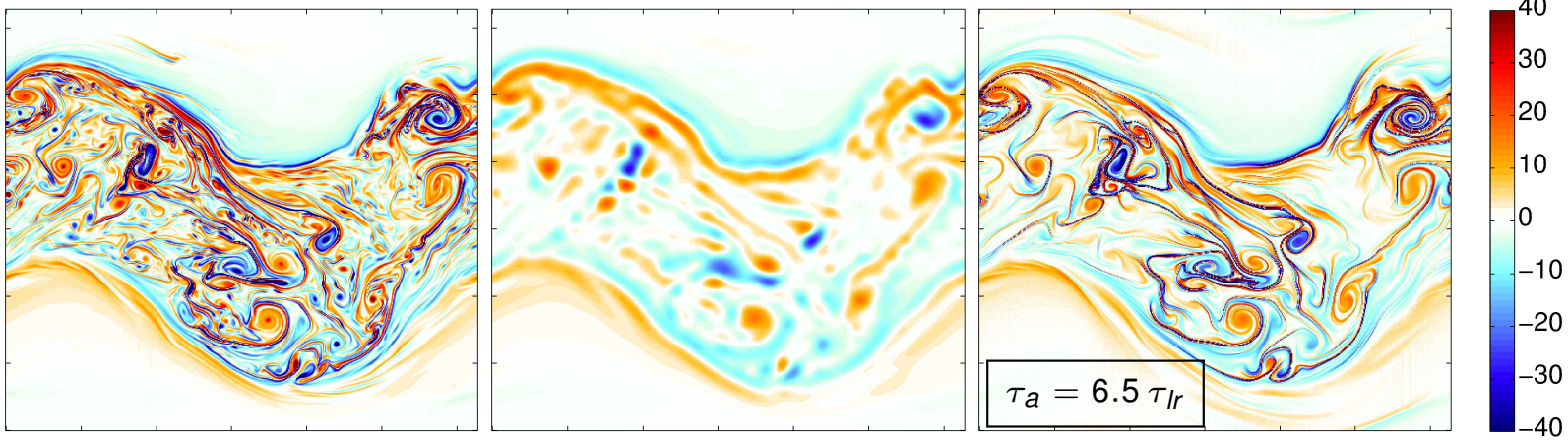

vorticity
at the surface
(horizontal flow)

$\zeta = (\partial_x v - \partial_y u)$
$= \nabla^2 \psi$

original; $t_0 = 50$ **degraded**; $t_0 = 50$ **reconstructed**; $t_0 = 50$

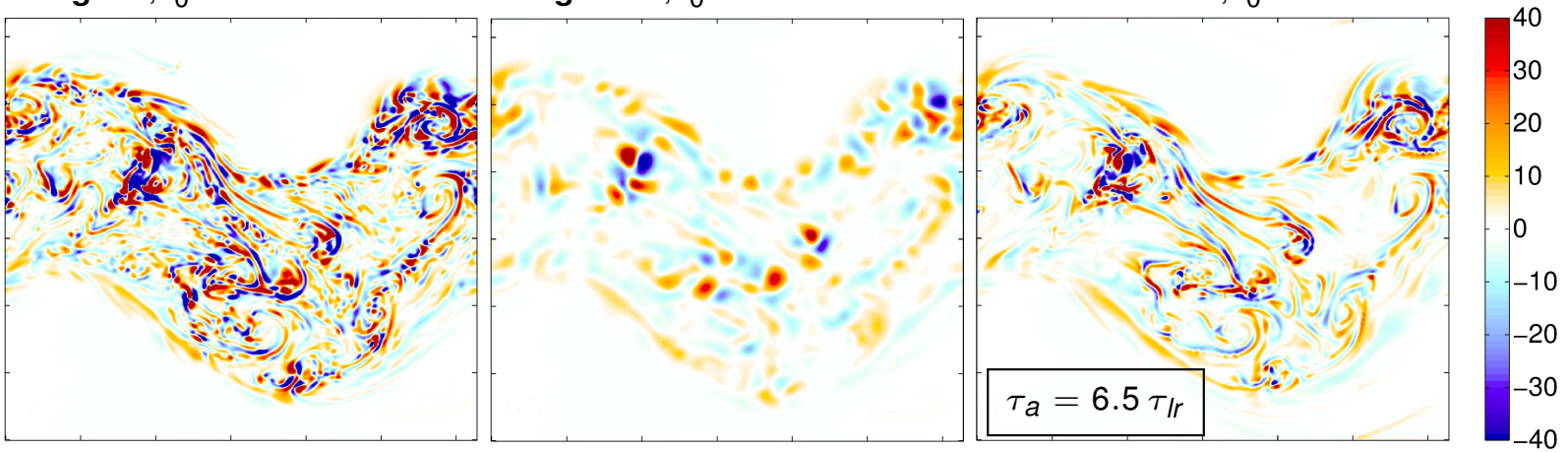

ageostrophic divergence
at the surface
(vertical flow)

$D = -\nabla \cdot \{\mathbf{u}\zeta +$
$+\mathcal{G}(k\mathcal{F}(\mathbf{u}\theta))\}$

Quantification of errors

Range of scales to be reconstructed $\longleftrightarrow$ $k_d < k < k_M$

Error computed from the spectrum of difference fields

$\theta_{hr} - \theta_{rec}$, $\zeta_{hr} - \zeta_{rec}$ for wavenumbers $k_d < k < k_M$

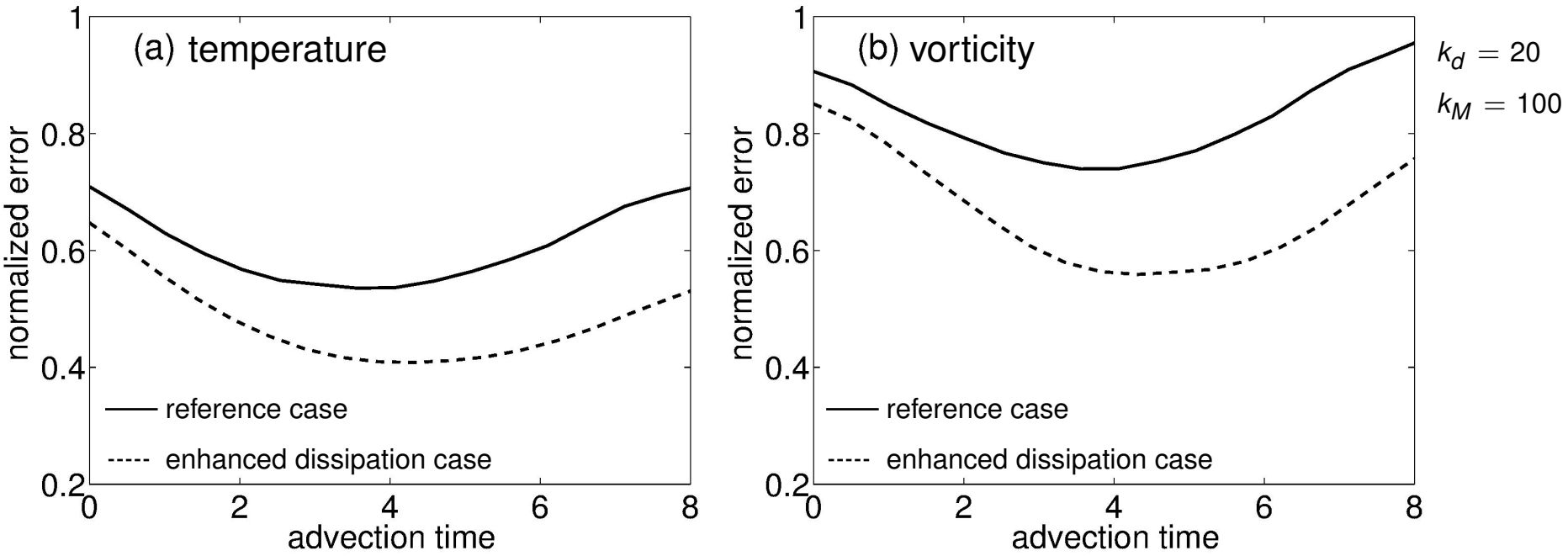

Not very large decrease but **minimum** for $\tau_a \approx (4-5)\,\tau_{lr}$

Conclusions

Lagrangian method for the reconstruction of tracer fields, like SST, at ocean surface. Coupling with SQG theory to reconstruct the velocity field.

1. Spatial patterns in high-resolution fields and in reconstructions: overall good agreement even in the presence of an external forcing.
   • Submesoscale filaments produced by the stretching by mesoscale eddies can be reconstructed. Their exact position is not good but it is possible to know in which region they are present.
   • Small intense eddies cannot be retrieved.
2. The method allows to reproduce the statistics of thermal fronts.
3. Optimal advection time for reconstructions $\tau_a \approx (4-5)\tau_{lr}$, reasonably corresponding to $\tau_a = (20-30)$ days, in regions of intense mesoscale activity.
4. Main limiting factors: (a) forcing on the transported tracer (SST), at large scale; (b) dynamical role of intense small structures, at small scale.

Perspectives on Lagrangian + SQG reconstructions

Possibility to improve the method through a kind of assimilation:

1. low-resolution temperature advected by low-resolution velocity
2. high-resolution temperature with associated high-resolution velocity (through SQG)
3. low-resolution temperature advected by new velocities

Perspectives: application to satellite data

high-resolution SST (AVHRR)

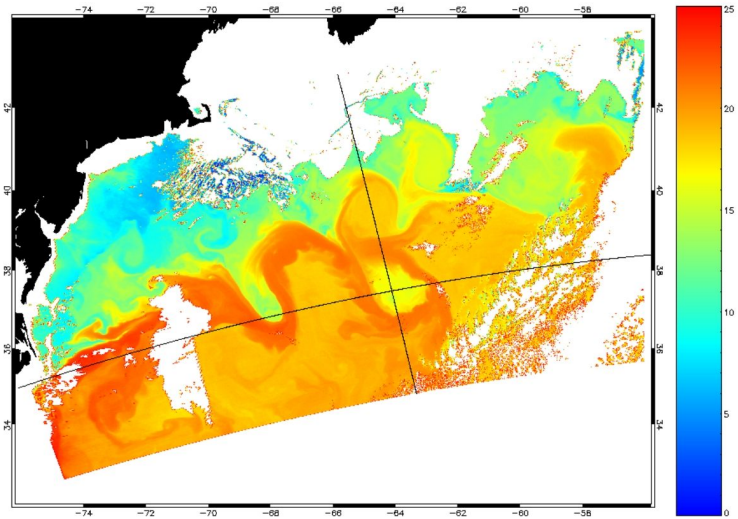

low-resolution SST (MW)

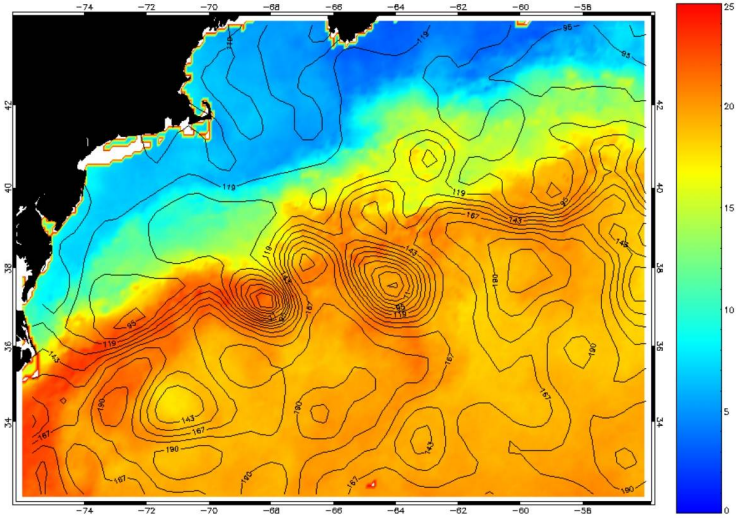

SST Lagrangian reconstruction

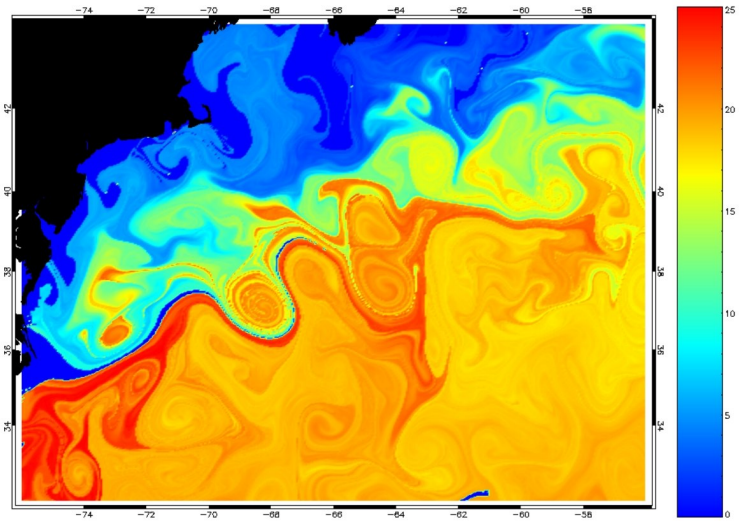

MW SST

SSH

$\tau_a = 15$ days

- from low-resolution SST
- velocity from SSH (by geostrophy)

Production of small scales in tracer fields

Evolution of tracer patches in mesoscale eddy field

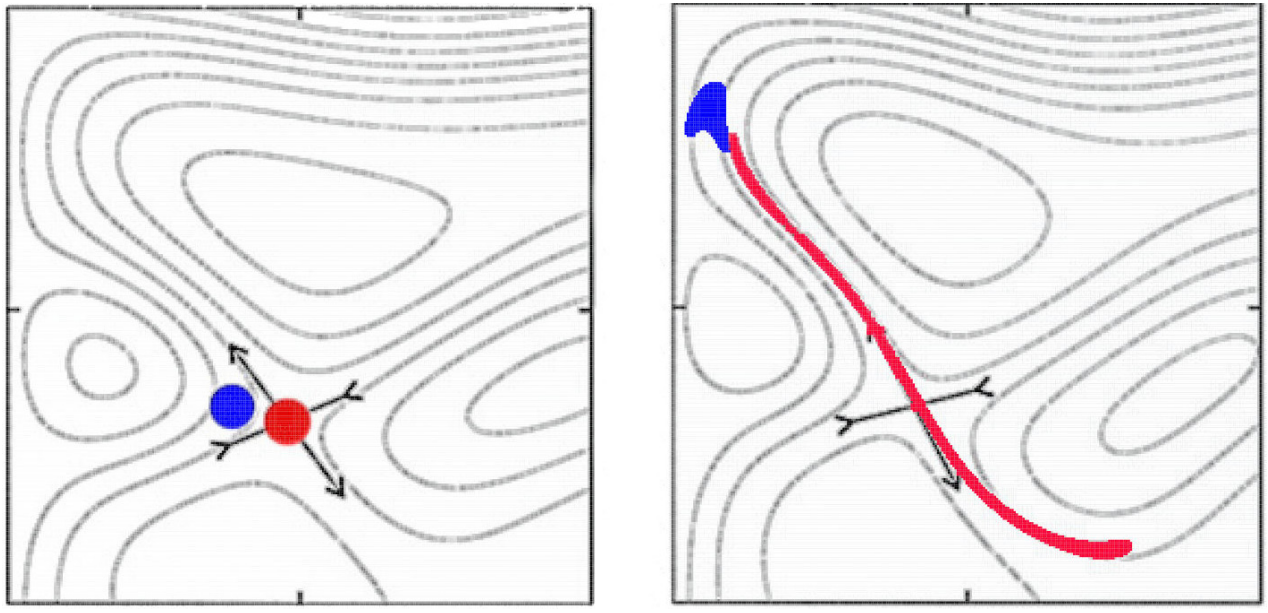

$$\frac{\partial C}{\partial t} + \boldsymbol{u} \cdot \boldsymbol{\nabla} C = 0$$

Lagrangian advection of tracers allows filamentation

Low-resolution tracer $\rightarrow$ high-resolution at a later time

Spectrum of temperature fluctuations

temperature fluctuation $\theta' = \theta - \langle\theta\rangle_x$; $\theta = \Theta - \beta y$

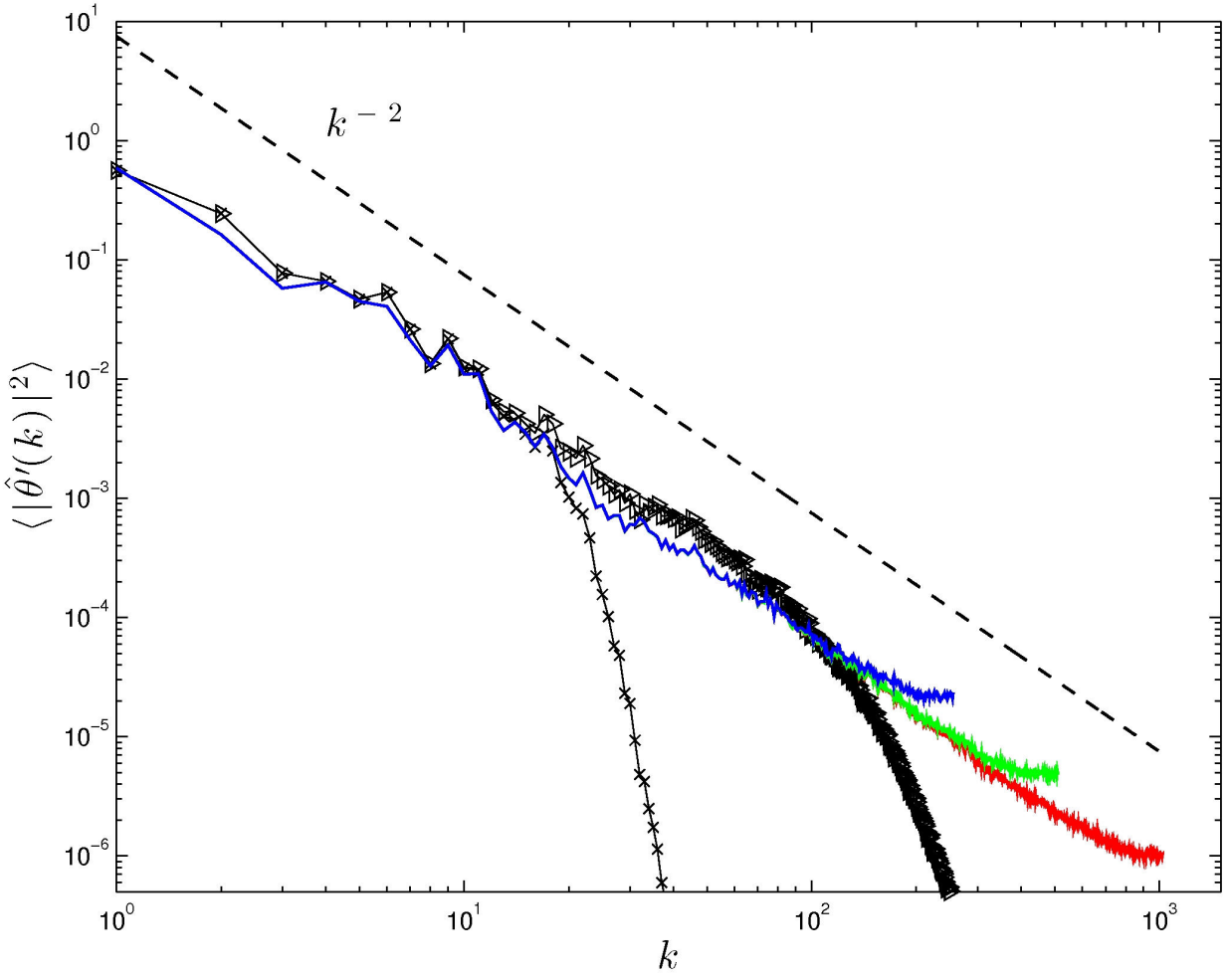

▷ original at t_0 ($N_{hr} = 512$)

× degraded at t_0

reconstructions with $\tau_a = 8\tau_{lr}$:

- $\sqrt{Np} = 512$
- $\sqrt{Np} = 1024$
- $\sqrt{Np} = 2048$

SQG: $\hat{\psi} = \hat{\theta}'/k \;\Rightarrow\; E(k) \propto \langle|\hat{\theta}'(k)|^2\rangle$ kinetic energy spectrum

Transects of SST

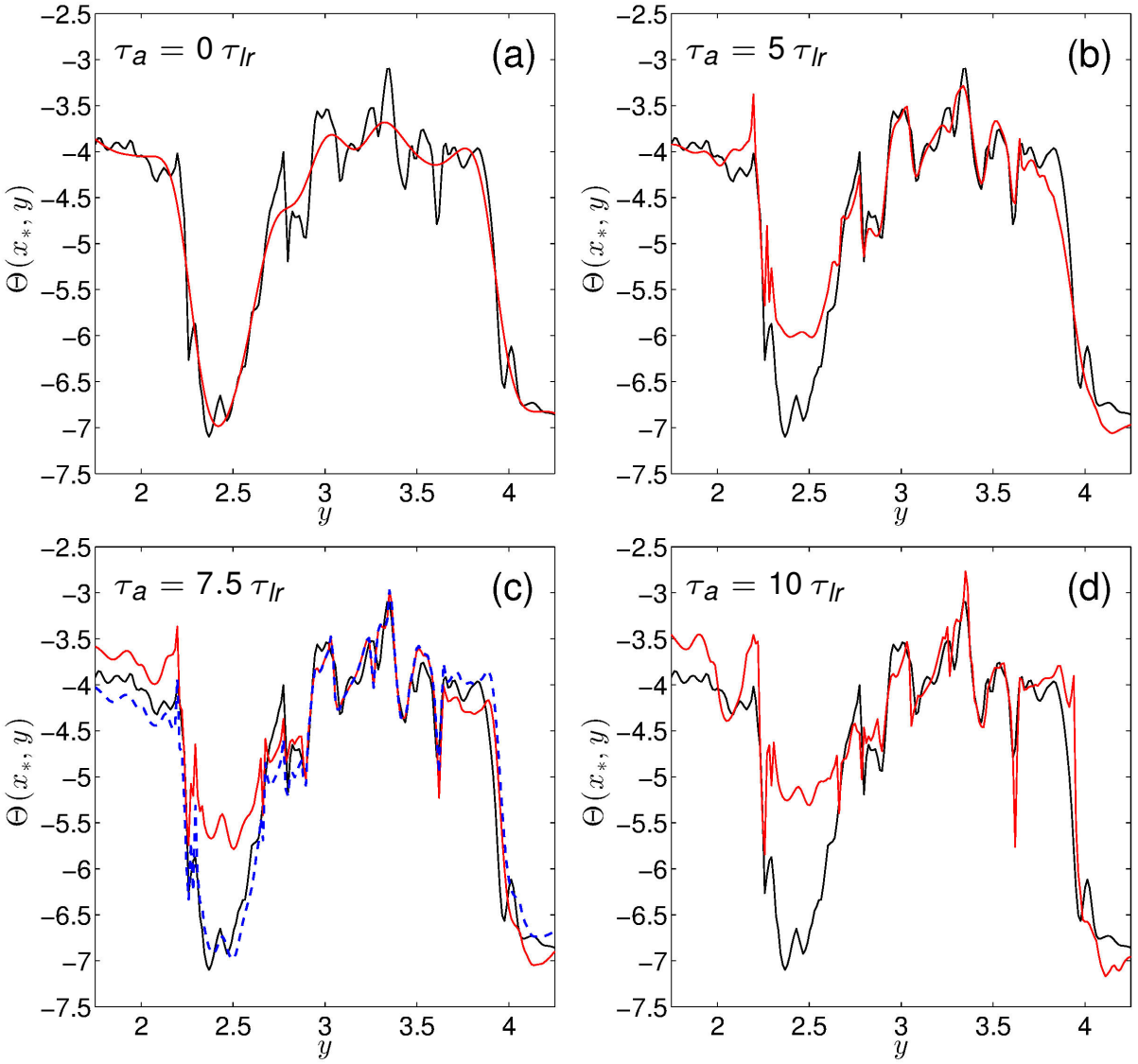

Meridional section of

$\Theta = \theta + \beta y$

at half domain width

$(x_* = \pi)$

SST original field

SST reconstruction

SST reconstruction with forcing